

A coplanar waveguide permeameter for studying high-frequency properties of soft magnetic materials

Y. Ding,^{a)} T. J. Klemmer, and T. M. Crawford^{b)}
Seagate Research, 1251 Waterfront Place, Pittsburgh, Pennsylvania 15222

(Received 18 December 2003; accepted 29 May 2004)

The high-frequency relative permeability of thin permalloy films was measured in the frequency and time domain using a microwave coplanar waveguide (CPW). Frequency domain measurements using a loop permeameter were performed for comparison. The Fourier transform of the time domain measurement, and the frequency domain measurement on the CPW agree closely, both showing a higher-frequency secondary resonance peak which is not seen with the loop measurement. This resonance likely arises from the lowest-order perpendicular standing spin wave mode of the permalloy film. © 2004 American Institute of Physics. [DOI: 10.1063/1.1774242]

I. INTRODUCTION

Increasing data rates in magnetic recording, as well as increasing frequencies in magnetic microwave devices, have pushed the operation frequency of magnetic materials to the GHz range. Techniques such as field-swept and frequency-swept ferromagnetic resonance,^{1,2} frequency-swept permeability measurement,^{3,4} and pulsed field magnetization rotation have been developed.⁵ Among these techniques, the apparatus for a frequency-swept permeameter (frequency domain measurement) and the step field magnetization rotation (time domain measurement) are easily implemented and place little restriction on the sample structure and geometry. The results of these techniques should be Fourier transforms of each other. However, in the past, measurements made on different apparatus have not yielded identical results, largely due to differences in methodology or equipment limitations.⁶ In this paper we present frequency domain measurements of NiFe films using a broadband coplanar waveguide (CPW) and a network analyzer. The same CPW and film are also used for time domain measurements, as described by Silva *et al.*⁵ For comparison purposes, frequency domain measurements were also performed on a permeameter with a single turn strip loop and a network analyzer, as described by Korovin *et al.*³ The results from all three techniques agree closely with each other in the low-frequency range, while at high frequencies, the measurements from the CPW (both time and frequency domain) show a minor resonance which is not seen in the loop frequency domain measurement.

II. EXPERIMENTAL SETUP

Figure 1(a) shows a schematic of the CPW permeameter. A network analyzer/S parameter test set with operating frequencies from 100 kHz to 6 GHz is used to measure the scattering parameters of a CPW with a thin film magnetic sample overlaying it. Both reflection (S_{11}) and transmission (S_{21}) coefficients are measured. The CPW is designed to

have near 50 Ω impedance, matching the network analyzer and cables. Two pairs of Helmholtz coils are used to supply magnetic fields up to 100 Oe either along or perpendicular to the CPW conductors. The center conductor of the CPW is 0.5 mm wide and generates a small in-plane rf magnetic field perpendicular to its axis. A thin film Ni₇₈Fe₂₂ sample on a Si substrate is placed on top of the CPW with the film side down. A thin layer of photoresist insulates the film from the CPW.

To make longitudinally-biased permeability measurements, the NiFe sample is placed with its easy axis along the CPW axis [Fig. 1(b)]. A saturating field is applied along the hard axis (in the direction of the rf field), and S_{11}^0 and S_{21}^0 are measured by the network analyzer over frequencies 100 MHz–6 GHz. Since S_{11}^0 and S_{21}^0 are measured with the film magnetically saturated, they contain information regarding only the nonmagnetic properties of the circuit. Next, the sample is saturated along its easy axis to erase the magnetic history of the sample. This field is then reduced to a desired

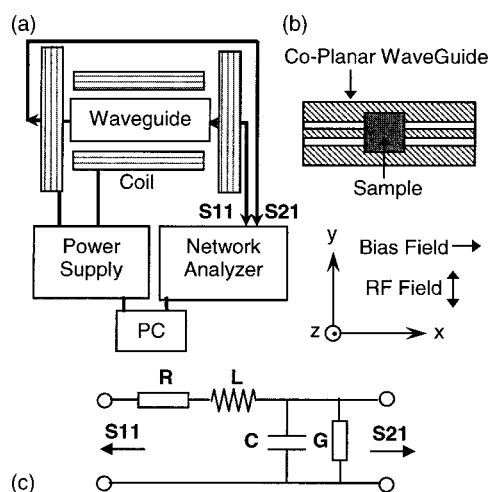


FIG. 1. Schematic of the coplanar waveguide (CPW) permeameter system (a) and an enlarged view of the waveguide (b) showing the location of the sample relative to the CPW. The equivalent circuit of a CPW section with a sample on the top is shown in (c), where L , R , C , and G are effective inductance, series resistance, capacitance, and shunt conductance, respectively. S_{11} and S_{21} are reflection and transmission coefficients.

^{a)}Present address: Department of Electrical and Computer Engineering, University of Minnesota, 4-174 EE/CSci building 200 Union Street S.E. Minneapolis, MN 55455.

^{b)}Electronic mail: thomas.m.crawford@seagate.com

value and the scattering factors S_{11}^1 and S_{21}^1 are measured. S_{11}^1 and S_{21}^1 contain information regarding both magnetic and nonmagnetic properties of the sample. Knowing these four parameters, the effective impedance arising from the sample magnetic response (i.e., permeability) of the sample can be determined.

To derive the change in characteristic impedance caused by the magnetic response of the film, the dielectric properties of the film and the substrate must be known. In spite of the attempt to match impedances, multiple reflections between the two ends of the sample must still be considered, given the weak size of the rf signal arising from the sample magnetics. To simplify the calculation, the part of the waveguide with a sample on top may be approximated as a lumped element with an effective inductance caused by the waveguide itself and film susceptibility (L), effective series resistance (R), shunt conductance (G), and capacitance (C), caused by the waveguide and sample substrate. The equivalent device circuit is shown in Fig. 1(c), and is the circuit for a two-wire transmission line.⁷ The reflection and transmission coefficients are

$$S_{11} = \frac{i\omega L + R + \frac{Z_0}{1 + Z_0(G + i\omega C)} - Z_0}{i\omega L + R + \frac{Z_0}{1 + Z_0(G + i\omega C)} + Z_0}, \quad (1)$$

$$S_{21} = \frac{2 \frac{Z_0}{1 + Z_0(G + i\omega C)}}{i\omega L + R + \frac{Z_0}{1 + Z_0(G + i\omega C)} + Z_0}, \quad (2)$$

where ω is the microwave angular frequency, and Z_0 is the characteristic impedance of the CPW (50 Ω). Solving for the reactance, using Eqs. (1) and (2), one obtains the simple relation,

$$i\omega L + R = \frac{1 + S_{11} - S_{21}}{1 - S_{11}} Z_0. \quad (3)$$

When the sample is saturated along hard axis, the rf field is parallel/antiparallel with the magnetization, and thus, $L = L_w$, where L_w is the self-inductance of the waveguide. The measured values are S_{11}^0 and S_{21}^0 . When the magnetization is along the easy axis with the rf field perpendicular to it, noting that $\chi \approx \mu$, where χ and μ are relative susceptibility and relative permeability, respectively, the effective inductance is

$$L \approx L_w + clt\mu\mu_0, \quad (4)$$

where l is the length of the film, t is the thickness of the film, c is a geometry factor with a dimension of m^{-1} , and μ_0 is the permeability of vacuum. Now the measured coefficients are S_{11}^1 and S_{21}^1 . Combining Eqs. (3) and (4), the relative permeability can be written as

$$\mu = \frac{Z_0 \left(\frac{1 + S_{11}^1 - S_{21}^1}{1 - S_{11}^1} - \frac{1 + S_{11}^0 - S_{21}^0}{1 - S_{11}^0} \right)}{icl\mu_0\omega}. \quad (5)$$

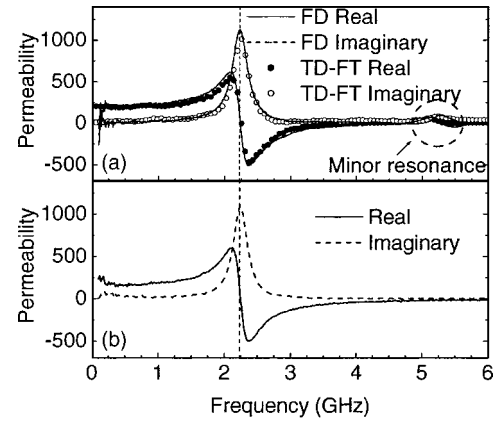


FIG. 2. (a) Relative permeability of $\text{Ni}_{78}\text{Fe}_{22}$ sample from coplanar waveguide frequency domain (solid and dotted lines) and time domain measurement (Fourier transform) (solid and open dots) with a longitudinal bias field of 50 Oe. (b) Relative permeability of the same sample from loop frequency domain measurement. The 100 nm thick $\text{Ni}_{78}\text{Fe}_{22}$ sample has $4\pi M_s$ of 1.1 T and H_k of 6.5 Oe.

The constant c is typically determined by measuring a standard sample with known initial relative permeability, and identical sample geometry (photoresist thickness, etc.), on the coplanar waveguide. As a result, the complex relative permeability can be calculated without knowing the values of the other circuit components. While there are few percent reflections at the connectors between the coaxial cable and the coplanar waveguide, these signals will subtract out of the permeability through the saturation/bias/subtraction process. While these weak reflections will also create an additional inductive response, this response will be a few percent compared with the measured inductive signal. As such, we expect this signal to be difficult to detect. Indeed, neither the frequency or time domain measurements show additional frequency peaks or phased signals suggesting the presence of these effects, justifying our neglect of these weak fields in analyzing the permeability spectra.

The time domain measurements are made using the same CPW used for the frequency domain measurement. However, the input to the CPW is replaced with a 10 V amplitude, 50 ps risetime, step pulse generator, and after the CPW, the step pulse is detected with a 20 GHz sampling oscilloscope.⁵ This pulse drives the magnetization out of equilibrium, creating a voltage that propagates along with the original step. Using the 20 GHz sampling oscilloscope, we detect 512–1024 averages at 100 kHz repetition rate, with the sample saturated by applying 100 Oe along the direction perpendicular to the CPW axis (sample hard axis). The averaged step pulse is then stored in memory. The sample is next saturated along the CPW axis to remove the field history, and finally, the field is reduced to the desired longitudinal bias field. A second averaged pulse is acquired, and the two pulses are subtracted to yield the inductive voltage created by the dynamic magnetization.⁵

III. RESULTS

The solid and dashed lines in Fig. 2(a) show the real and imaginary parts of the relative permeability spectrum for a 100 nm thick $\text{Ni}_{98}\text{Fe}_{22}$ film at a bias field of 50 Oe. The

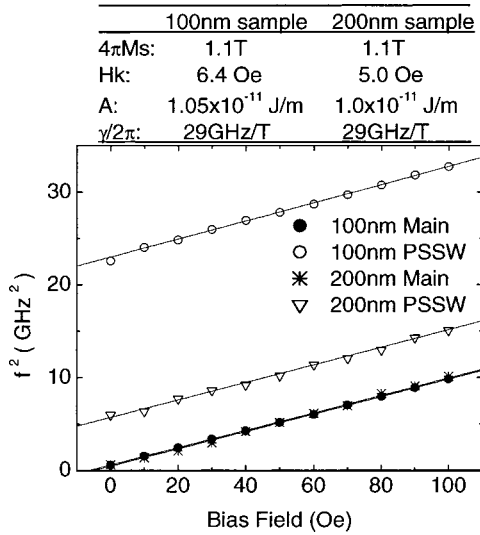


FIG. 3. Frequency squared of primary and secondary resonance frequencies vs bias field. Solid lines are calculations using parameters listed in the table, assuming the primary resonance is the uniform mode and the secondary resonance is a perpendicular standing spin wave (PSSW) mode, with mode index $p=1$.

circles in Fig. 2(a) show the real and imaginary parts of a Fourier transformed time domain measurement for the same sample and CPW. The time domain spectra are normalized to the dc response, and then scaled by the initial relative permeability of the reference sample, as mentioned above. The two measurements yield identical spectra. The close agreement between the frequency and time domain measurements indicates that the LCR equivalent circuit shown in Fig. 1(c) is a good approximation to the coplanar waveguide with a magnetic film on the top.

Figure 2(a) shows a second resonance peak at $f = 5.25$ GHz. This peak appears in both frequency and time-domain data. Figure 2(b) shows equivalent data obtained with the loop permeameter, and the second resonance peak is absent from the loop data. To ascertain whether the second resonance is something systematic with the coplanar waveguide, we measured its frequency as a function of magnetic field, as shown in Fig. 3, where we plot frequency-squared versus bias field. The open circles are for the second resonance, while the solid circles represent the primary resonance. Both peak frequencies, squared, are linear in applied field, suggesting the second resonance is of magnetic origin.

To further confirm this observation, we measured a 200 nm thick NiFe film to compare with the 100 nm film. The second resonance is still present, but at a lower frequency (open triangles in Fig. 3). However, the main resonance frequency for the 200 nm film is identical to that of the 100 nm film (asterisks). Given the inverse frequency dependence on thickness, coupled with discussions regarding spin wave modes observable with coplanar waveguides,⁸ we calculate the predicted frequencies for perpendicular standing spin waves (PSSW) as follows:⁹

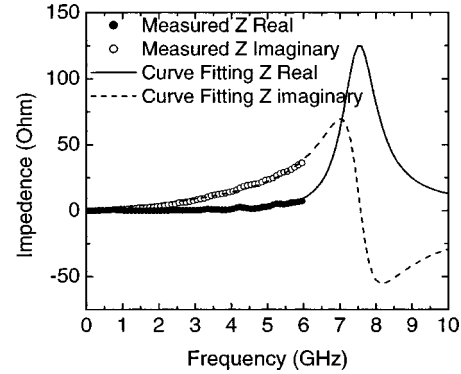


FIG. 4. Measured loop impedance values and calculated results using LCR model for the loop permeameter.

$$f_p = \frac{\gamma}{2\pi} \left(\left[H + H_k + \frac{2A}{M_s} q_{\parallel}^2 + \frac{2A}{M_s} \left(\frac{p\pi}{d} \right)^2 \right] \times \left\{ H + H_k + \left[\frac{2A}{M_s} + H \left(\frac{4\pi M_s d}{p\pi H} \right)^2 \right] q_{\parallel}^2 + \frac{2A}{M_s} \left(\frac{p\pi}{d} \right)^2 + 4\pi M_s \right\} \right)^{1/2}, \quad (6)$$

where γ is the gyromagnetic ratio, A is the exchange constant, d is the film thickness, q_{\parallel} is in-plane wave vector, p is perpendicular standing spin wave number ($p=0$ for main resonance and $p=1$ for the PSSW of the first order), H_k is the uniaxial anisotropy, and H and M_s are applied dc field and saturation magnetization, respectively. We note that Eq. (6) was derived using the condition of unpinning spins at the top and bottom surfaces of the film. In our calculation we assume long in-plane wavelength and neglect all the q_{\parallel} terms. The solid lines in Fig. 3 are fits to the data, using the parameters in the table above Fig. 3 (varying A and H_k). The agreement between measured and predicted frequencies is quite good, and the fitted exchange constant, A , and uniaxial anisotropy, H_k , are close to typical values for NiFe films. These results suggest the conclusion that the minor resonance is the $p=1$ PSSW mode of these films.

The impedance of the loop permeameter with a saturated sample was also measured. Figure 4 shows the measured loop impedance and a calculation using a LCR model.¹⁰ Fitting the data in Fig. 4 implies that our loop has an intrinsic resonance frequency of ~ 7.5 GHz, as the model and measurement agree closely to $f=6$ GHz. However, the 6 GHz network analyzer frequency limit makes this intrinsic resonance more difficult to fit quantitatively. The electrical resonance is caused by the intrinsic coil structure of the loop, and it can only be pushed to limited higher frequencies by using a low dielectric constant substrate or changing the geometry of the coil. However, for the coplanar waveguide measurement, the magnetic film can be directly deposited on top of the center strip line, and the operation frequency is determined by the bandwidth of the waveguide itself. Therefore the coplanar waveguide can be used for permeability measurements to much higher frequencies.

The absence of the $p=1$ PSSW mode in the loop measurement is not caused by reduced loop bandwidth as com-

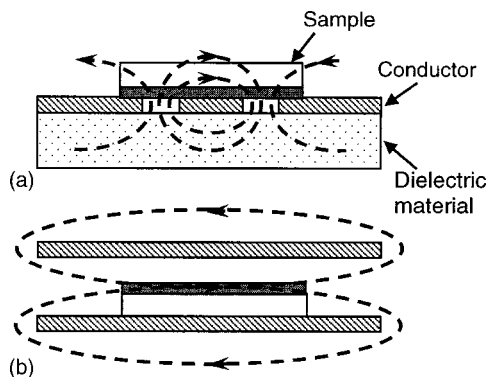


FIG. 5. Schematic of magnetic field distributions for a coplanar waveguide (a) and a loop permeameter (b). The broken lines represent the magnetic field of the current carrying wires. Note that the field distribution is spatially inhomogeneous over the sample for the coplanar waveguide source and uniform for the loop source.

pared to the CPW, because the 200 nm PSSW mode has frequencies ranging from 2–4 GHz, depending on H_b , which is well within the loop bandwidth. Therefore, we look for other differences between the excitation sources. One difference is that the excitation field in the CPW case is spatially inhomogeneous, compared with the uniform field of the loop permeameter, as illustrated in Fig. 5. This difference in spatial field distribution may explain the presence of the PSSW mode in the CPW data but not in the loop data. Without any surface pinning, PSSW modes are seen only for nonuniform excitation fields.^{11–13} If the spins at the two surfaces of the film experience a different anisotropy than the spins inside the film (partially or fully pinned), then a uniform field can excite a PSSW mode.^{11,13} Obviously, particular combinations of partial surface pinning with field inhomogeneity could also generate PSSW modes. Additional study is required to

elucidate the exact nature of the PSSW modes in these films, including the degree of surface pinning, if any. The ability to detect such dynamical magnetization effects is an advantage to using the CPW technique. That spin waves are observed in both frequency and time domain data for the same film strengthens the argument that time and frequency domain techniques may be used interchangeably to yield identical results for thin film magnetization dynamics.

ACKNOWLEDGMENTS

One of the authors (Y.D.) wishes to thank C. Alexander and J. Rantschler for helpful discussions on loop permeameter measurements.

- ¹M. Prutton, *Thin Ferromagnetic Films, and References Therein* (Butterworth, Washington, 1964), p. 193.
- ²M. E. Unwin, P. W. Haycock, S. R. Hoon, and P. K. Grannell, *J. Magn. Magn. Mater.* **205**, 199 (1999).
- ³V. Korenivski, R. B. van Dover, P. M. Mankiewich, Z. X. Ma, A. J. Becker, P. A. Polakos, and V. J. Fratello, *IEEE Trans. Magn.* **32**, 4905 (1996).
- ⁴M. Yamaguchi, S. Yabukami, and K. I. Arai, *IEEE Trans. Magn.* **33**, 3619 (1997).
- ⁵T. J. Silva, C. S. Lee, T. M. Crawford, and C. T. Rogers, *J. Appl. Phys.* **85**, 7849 (1999).
- ⁶C. Alexander, J. Rantschler, T. J. Silva, and P. Kabos, *J. Appl. Phys.* **87**, 6633 (2000).
- ⁷R. E. Collin, *Foundations for Microwave Engineering* (McGraw-Hill, New York, 1992), p. 86.
- ⁸T. J. Silva (private communication).
- ⁹J. Jorzick, S. O. Demokritov, C. Mathieu, B. Hillebrands, B. Bartenlian, C. Chappert, F. Rousseaux, and A. Slavin, *Phys. Rev. B* **60**, 15194 (1999).
- ¹⁰D. Pain, M. Ledieu, O. Acher, A. L. Adenot, and F. Duverger, *J. Appl. Phys.* **85**, 5151 (1999).
- ¹¹C. Kittel, *Phys. Rev.* **110**, 1295 (1958).
- ¹²R. L. White and Irvin H. Solt, Jr. *Phys. Rev.* **104**, 56 (1956).
- ¹³R. Weber, *IEEE Trans. Magn.* **4**, 28 (1968).